

JMAPS Technical Memoranda 10-03

Sub-Pixel Phase Error Analysis

Zack Dugan

zachary.dugan@usno.navy.mil

22 July 2010

ABSTRACT

We analyze the sub-pixel phase error on JMAPS centroiding for 20 second exposures of 12^{th} magnitude I-band F5, O5, and M5 type stars. We calculate the observed minus true positions of simulated stars based on JSIM polychromatic PSF fits for specific spectral types. For three different spectral types, we show the mean, standard deviation, and standard deviation of the mean of the pixel phase errors for both the x and y dimensions as a function of the number of observations before correction. We use interpolated 2D pixel offset maps to make the initial correction, and then a 1D average residual function for the second correction. We find that the sub-pixel phase error reduces as the square root of the number of observations, and further that it can be corrected to such a high degree that its contribution to the total error will likely be negligible.

1. Methodology and Data

Understanding and correcting sub-pixel phase error is critical to meet JMAPS precision and accuracy requirements. Using JSIM, we select random pixel locations (integer and decimal) between the 10th and 20th pixels on a 40 by 40 pixel grid for 72, 20 second exposures of 12^{th} magnitude I-band F5, O5, and M5 type stars. For example in an (x,y) pixel location format, we may select (10.01, 19.8) or (12.3, 15.0). Varying over these pixels is sufficient to analyze sub-pixel phase error. We then simulate the centroiding errors in pixels in x and y on each of the 72 random locations. We repeat the 72 observations for 100 iterations. We initially calculate two methods of correcting sub-pixel phase error: the first using a one-dimensional sinusoidal algorithm, and the second using a comprehensive, two-dimensional sub-pixel phase error map over the entire grid. Then we use interpolated sub-pixel phase error maps followed by 1D corrections for the best reduction in sub-pixel phase error.

1.1. Initial Methods

Figure 1 shows uncorrected scatter plots of the x centroiding errors (in pixels) vs. the y centroiding error (in pixels) over the 100 iterations of 72 observations for an O5, F5, and M5 type star.

We then take the uncorrected x and y centroiding pixel errors for the first of the 100 iterations and plot them as a function of their sub-pixel location in Figure 2. We use a classic sinusoidal least squares fit to model the centroiding error as a function of sub-pixel location, and these models are also shown in Figure 2. However, both x and y sinusoidal models leave residual errors, as shown by the vertical spreads in the centroiding errors for each sub-pixel location. Therefore, the sinusoidal fits are rejected, and comprehensive, two-dimensional sub-pixel phase error maps are created for all three spectral types with the maximum possible resolution of 2500 sub-pixel locations, shown in Figure 3. Figure 4 shows the total pixel error as a function of sub-pixel location for all three spectral types and the corresponding vector offset maps. The maps shown in Figure 4 were calculated by adding the x and y sub-pixel error maps from Figure 3 in quadrature.

After correcting for sub-pixel phase error with the comprehensive two-dimensional maps, shown in Figure 3, by subtracting the sub-pixel phase error map value from the initial centroided pixel, some residual errors remain. Figure 5 compares the uncorrected error scatter plots to the initially corrected residual error scatter plots. These residual errors are shown as a function of sub-pixel location in Figure 6. Tables 1 shows the statistics after 72 observations for the uncorrected and initially corrected results using the 50x50 pixel error maps.

Table 1: Spectral Types and Initially Corrected Pixel Phase Error Statistics after 72 Observations

Spectral Type	Mean X Pixel Error	Mean Y Pixel Error	StanDev of X Pixel Error	StanDev of Y Pixel Error	StanDev of Mean X Pixel Error	StanDev of Mean Y Pixel Error
O5	-0.00025	-0.00016	0.00192	0.00184	0.00020	0.00023
F5	-0.00033	-0.00013	0.00216	0.00203	0.00030	0.00025
M5	-0.00026	-0.00006	0.00224	0.00213	0.00025	0.00025

1.2. Investigating Residual Discontinuities

After initial correction with the comprehensive 50x50 pixel error maps, the residual errors left behind show discontinuities as a function of sub-pixel location, as shown in Figure 6. These discontinuities were first thought to be a result of limited map resolution and sub-pixel location. Figure 7(a) and (b) show the discontinuous residual errors as a function of

sub-pixel location color coated as a function of error magnitude with channels highlighting the discontinuous areas. The rest of the analysis of this Technical Memorandum focuses on the M5 because it is the worst case scenario. Under the same color scheme, and otop the pixel offset map for an M5, we show the actual pixel locations, JSIM initial guesses¹, and final JSIM centroided pixel locations with the discontinuous residual X errors in Figure 7(c)-(e). We also investigate the gradient maps as the source of the discontinuities, showing the actual pixel locations otop the X gradient map of the pixel error map, the X gradient map of the X gradient map, and the Y gradient map of the X gradient map in Figure 7(f)-(h). Figure 11 shows the same information for discontinuous residual Y pixel errors. From these results, no unifying underlying characteristics stand out about the discontinuous regions. However, if limited sub-pixel resolution were a large contributing factor, then interpolation to a higher resolution would solve the issue.

1.3. Interpolation and Second Correction

Several methods of interpolation are investigated: Python Congrid Linear, Python Congrid Neighbor, Python Congrid Spline, IDL Congrid Cubic with the Cubic Parameter set to 0, -0.5, and -1., and IDL Congrid Linear. Interpolations were done on the 50x50 pixel error maps to create 5000x5000 high resolution pixel error maps. IDL Congrid Cubic with the Cubic Parameter set to -0.5 created the best results. Figures 9(a)-(d) show the original and interpolated maps. Figures 9(e)-(h) show residual errors as a function of sub-pixel location after correction with the original and interpolated pixel error maps. Figures 9(i) and (j) show residual error plots after correction with the original and interpolated pixel error maps.

The important difference in results is that the residual errors as a function of sub-pixel location go from discontinuous after correct with the original pixel error maps to continuous after correction with the interpolated pixel error maps. While the residuals themselves are not significantly smaller than before, because they are continuous as a function of sub-pixel location, they can easily be modeled and subtracted. Figure 10(a) shows the residual X pixel error for an M5 after correction with the interpolated pixel error map, as well as sinusoidal, average, and 5th, 6th, and 7th order polynomial fits to the data. The average fit is generated by calculating the mean of all residuals in a 0.01 pixel bin of sub-pixel location, and is the most accurate model of residual errors after correction with the interpolated sub-pixel error maps. In Figure 10(b), we show the residual pixel errors after second correction with the average fit, color coated by second residual error pixel location. In Figure 10(c), in the same

¹JSIM initial guess refers to the location where JSIM initially places the PSF.

colors, we show the actual pixel locations of the outlier second residual pixel error locations. In Figures 10(d) and (e), in the same colors, we show the X and Y second residual pixel errors as a function of sub pixel location. Statistics for an M5 twice corrected with the interpolated pixel phase error map and average residual fit after 72 observations are shown in Table 2.

Table 2: Spectral Types and Second Corrected Pixel Phase Error Statistics after 72 Observations

Spectral Type	Mean X Pixel Error	Mean Y Pixel Error	StanDev of X Pixel Error	StanDev of Y Pixel Error	StanDev of Mean X Pixel Error	StanDev of Mean Y Pixel Error
M5	0.00004	0.00004	0.00066	0.00059	0.00016	0.00014

Note: These statistics generated after correction with an interpolated pixel error map and an average residual subtraction.

2. Analysis

2.1. Asymmetric Errors

The asymmetric grouping of x and y pixel errors shown in Figure 1 is attributable to the asymmetry of the pixel magnitude offset, as shown in Figure 3. These pixel magnitude offsets make centroiding errors more likely to occur in certain directions, causing asymmetry in the resulting errors. The residual x and y pixel errors as a function of sub-pixel location, as shown in Figure 8, are also a result of the asymmetry of the pixel magnitude offset. The discontinuous curve is explained by the upper limit to sub-pixel phase error correction. JSIM can only correct with the comprehensive two dimensional pixel error map as accurately as the initial centroided values are. JSIM uses the initial centroided value calculated with no correction to determine the sub-pixel location and corresponding sub-pixel phase error map value. Thus, errors in the initial centroided value, which are inevitable, cause an error in the returned corrected value from the correction map. This process can cause discontinuity in the residual pixel error depending on the sub-pixel location, as shown in Figure 6.

2.2. Statistics and Final Numbers

After sub-pixel correction, the standard deviation over all iterations of the mean residual pixel errors as a function of number of observations falls as $1/\sqrt{\#observations}$, as expected.

After, sub-pixel phase error corrected with the two dimensional maps, we see vast improvement in the centroiding error. However, the remaining error we see spreads over about 0.004 pixels, from -0.002 to 0.002 pixels in both x and y as shown in Figure 10(b). After

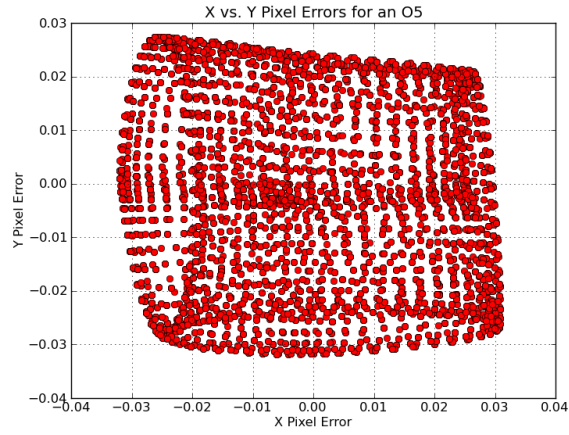
72 observations, we can expect a maximum centroiding offset of around 0.0004 pixels in any direction, corresponding to roughly 0.16 milliarcseconds (mas), after sub-pixel phase error correction.

3. Summary

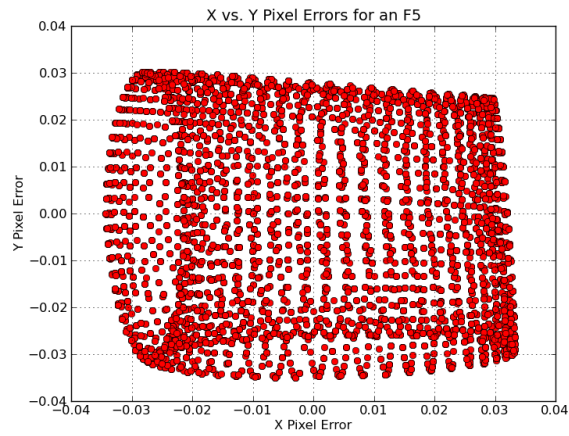
We use comprehensive, two dimensional interpolated sub-pixel phase error maps in combination with an average residual fit to correct for sub-pixel centroiding error. We find that the standard deviation of the mean residual pixel errors falls as $1/\sqrt{\#observations}$, as expected. We also find that our method is highly effective in correcting this error, reducing the standard deviation of the mean sub-pixel offset to 0.087 mas after 72 observations in both the x and y directions. Furthermore, the reduction in sub-pixel phase error is large enough that this error will likely be negligible when combined with other factors contributing to the total centroiding error.

4. References

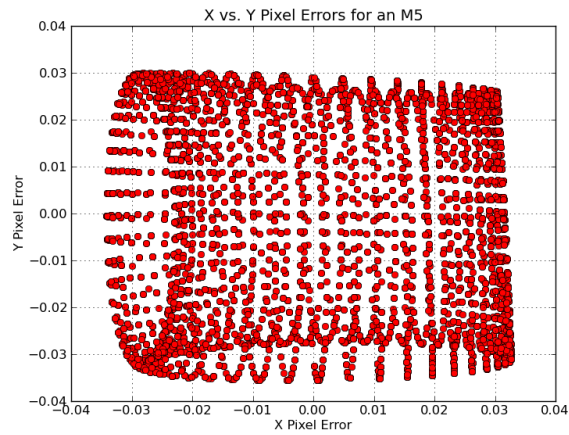
Veillette, D. 2009, JSIM.



(a)

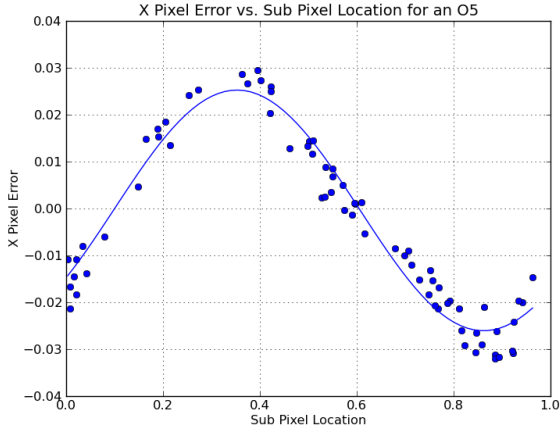


(b)

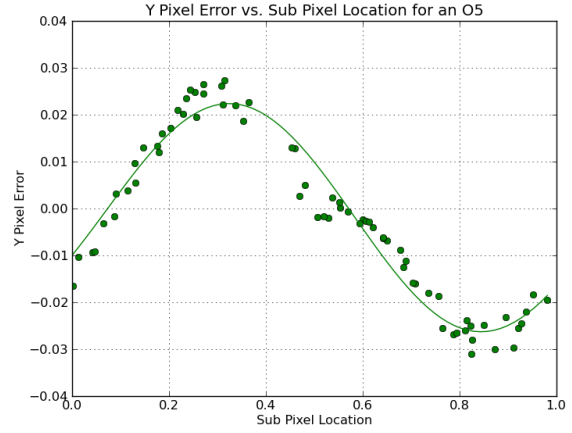


(c)

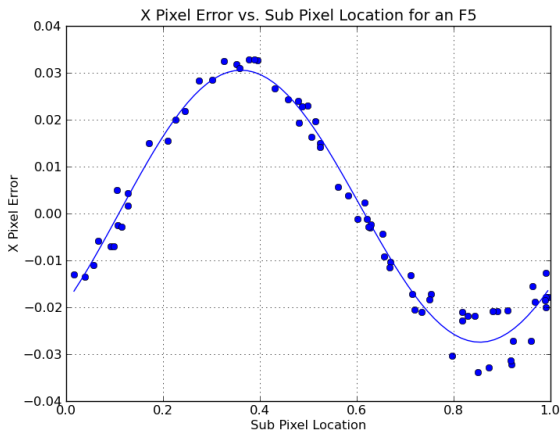
Figure 1: Uncorrected Pixel Errors in X and Y for a 20s Exposure of a 12^{th} magnitude O5, F5, and M5 in a, b, and c, respectively



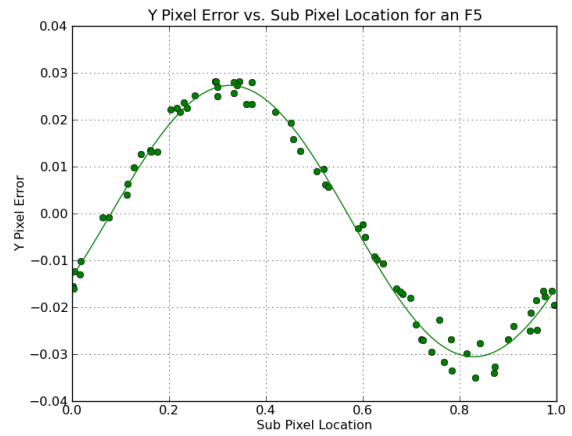
(a)



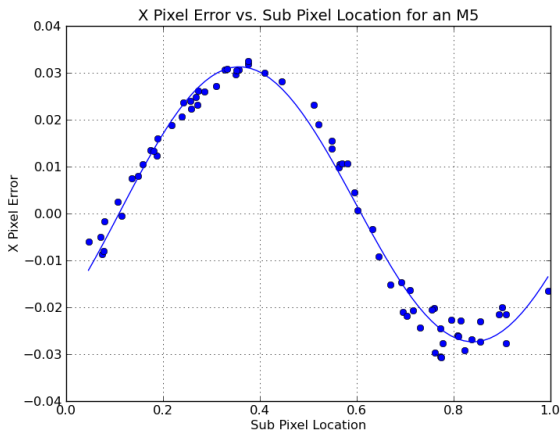
(b)



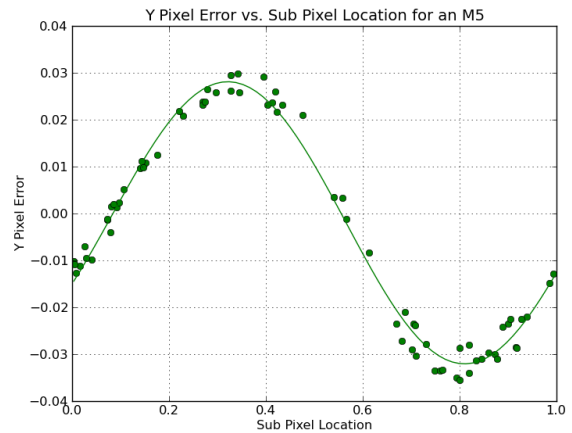
(c)



(d)

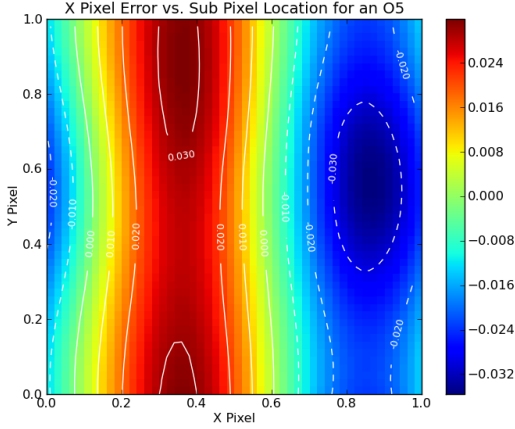


(e)

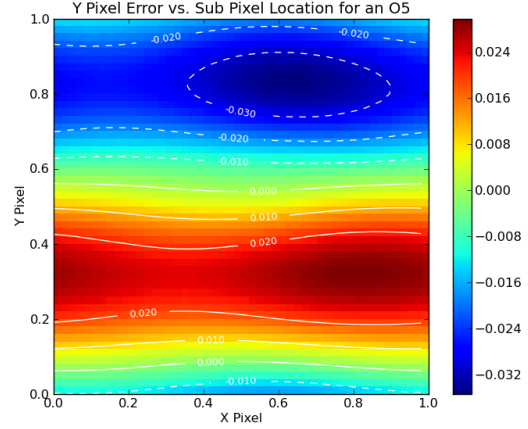


(f)

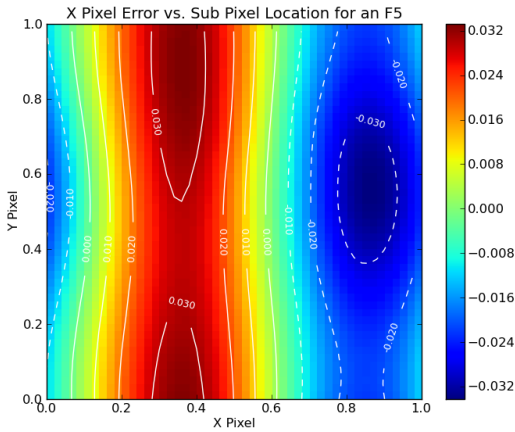
Figure 2: Pixel Errors and Fits vs. Sub-Pixel Location in X and Y for a 20s Exposure of a 12th magnitude O5, F5, and M5



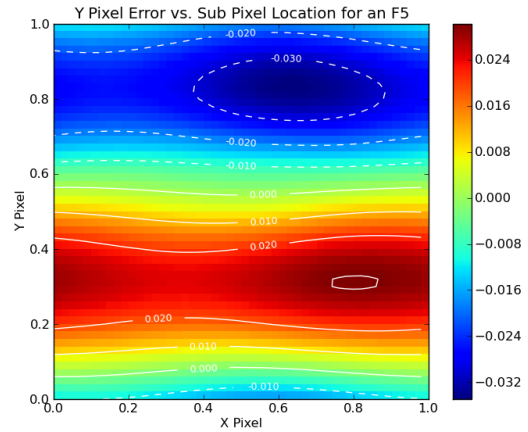
(a)



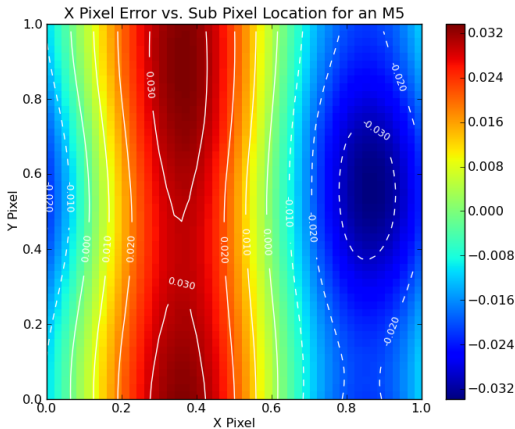
(b)



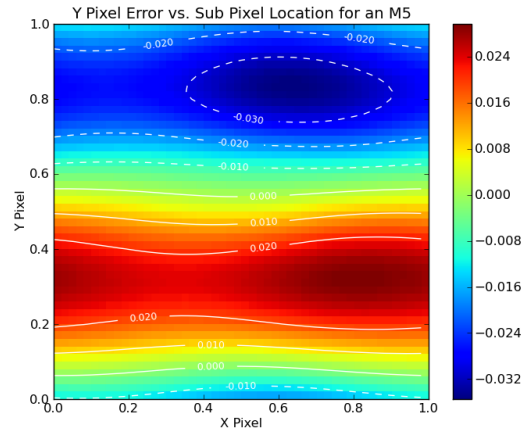
(c)



(d)

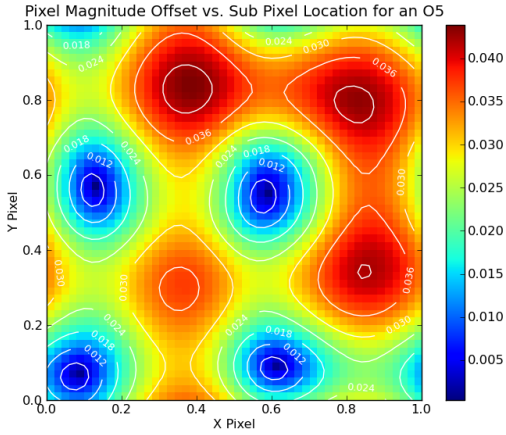


(e)

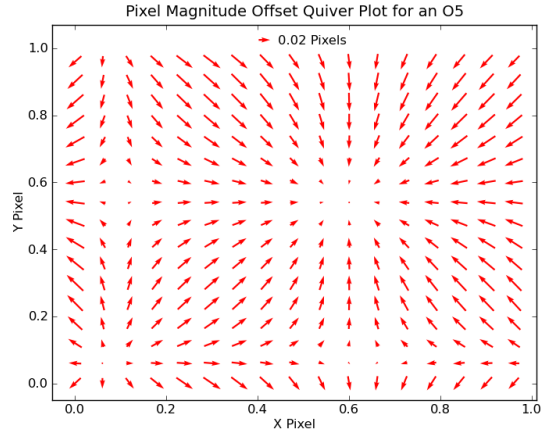


(f)

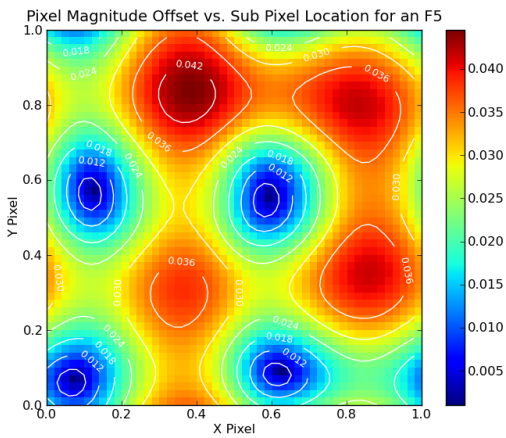
Figure 3: 50x50 and 500x500 Interpolated Sub-Pixel Phase Error Maps in Y for a 20s Exposure of a 12th magnitude O5, F5, and M5



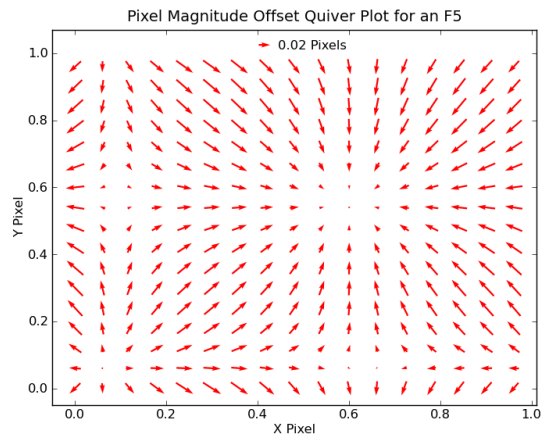
(a)



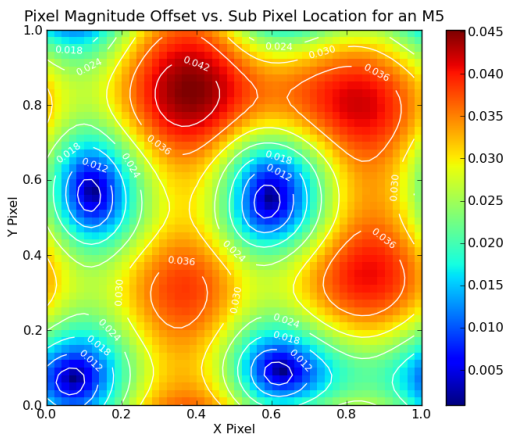
(b)



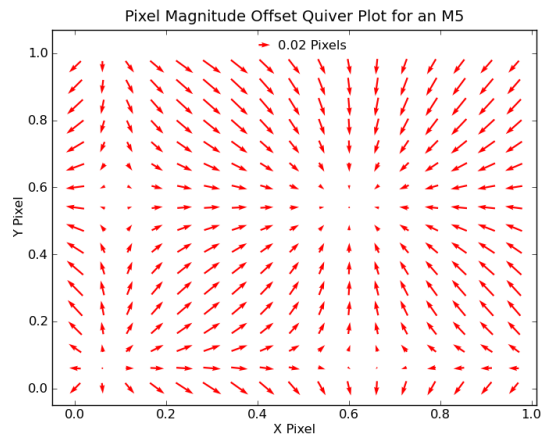
(c)



(d)

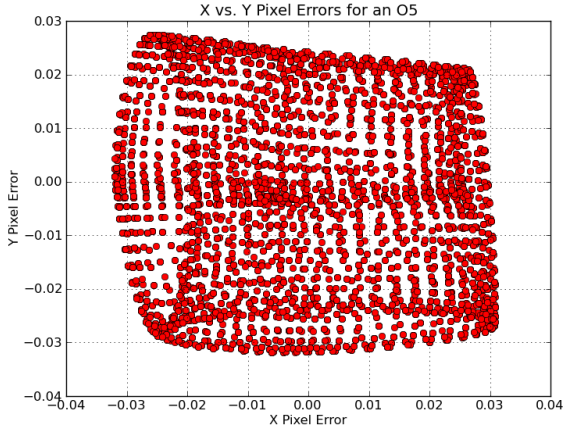


(e)

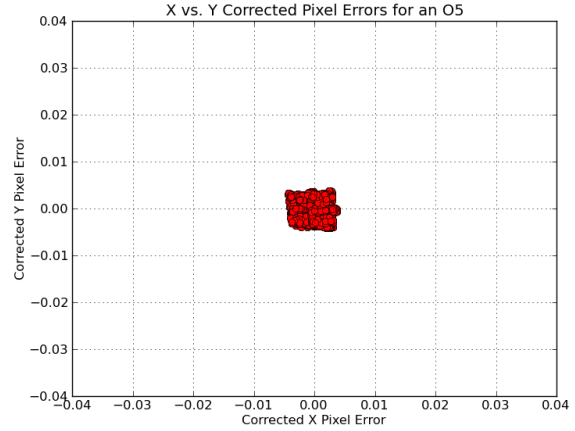


(f)

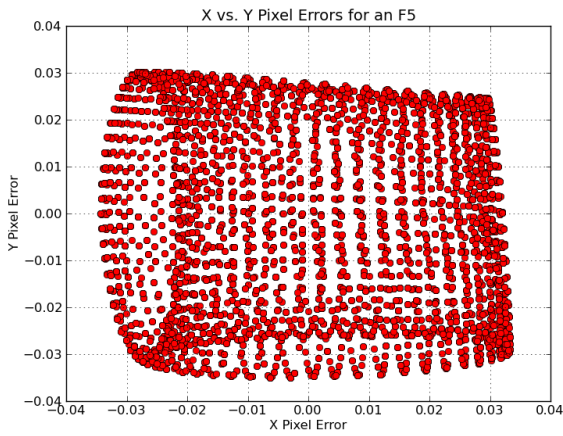
Figure 4: 50x50 and 500x500 Interpolated Sub-Pixel Phase Error Maps in Y for a 20s Exposure of a 12th magnitude O5, F5, and M5



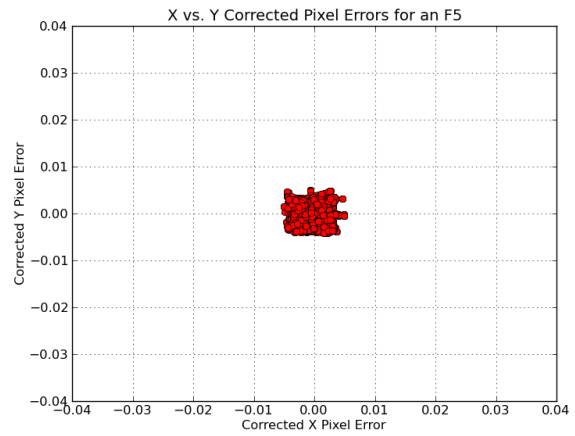
(a)



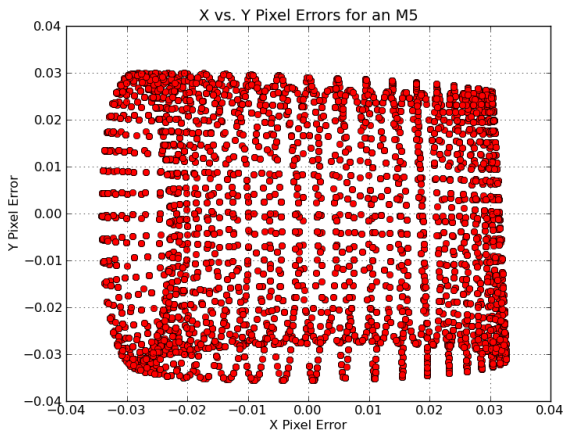
(b)



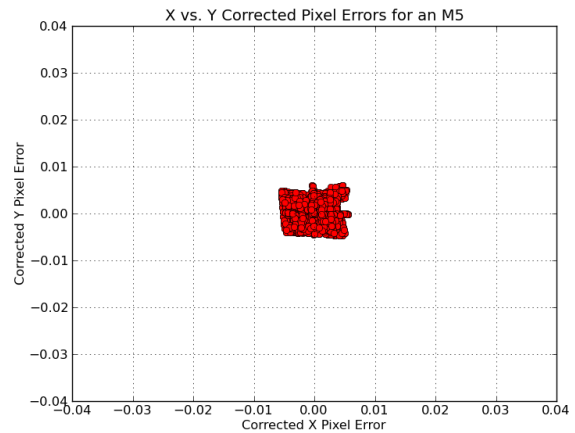
(c)



(d)

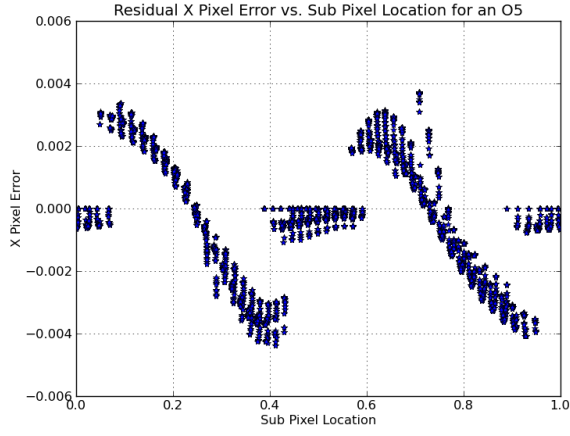


(e)

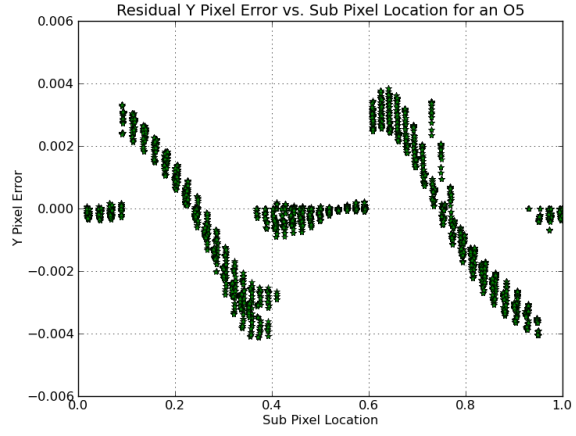


(f)

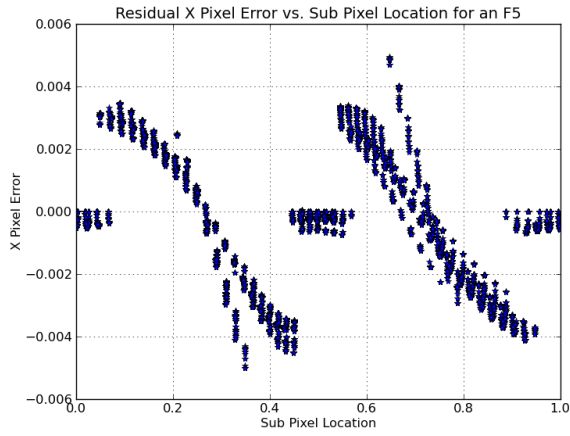
Figure 5: Uncorrected and Corrected Pixel Errors in X and Y for a 20s Exposure of a 12th magnitude O5, F5, and M5 in a, b, and c, respectively



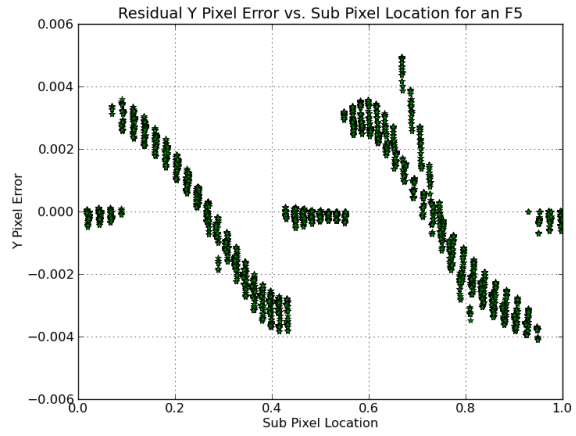
(a)



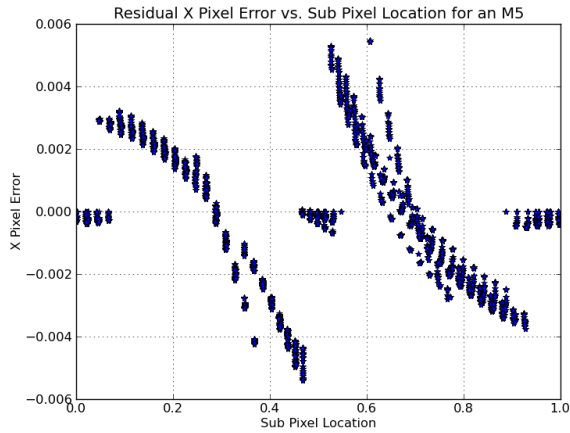
(b)



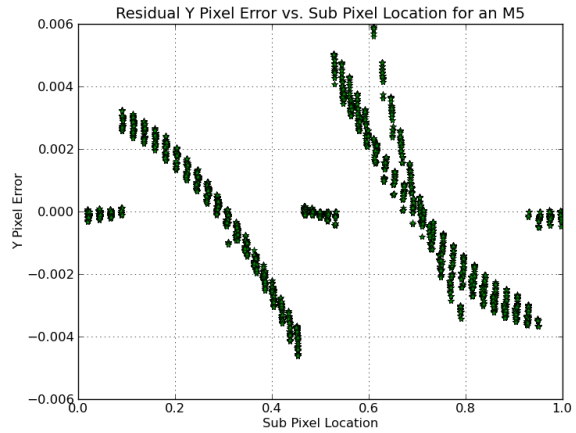
(c)



(d)

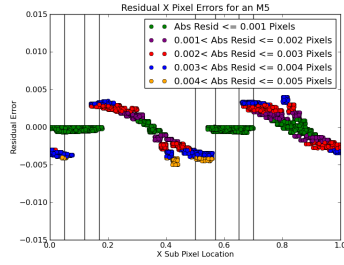


(e)

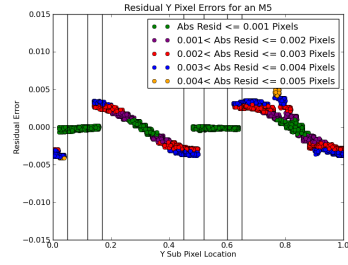


(f)

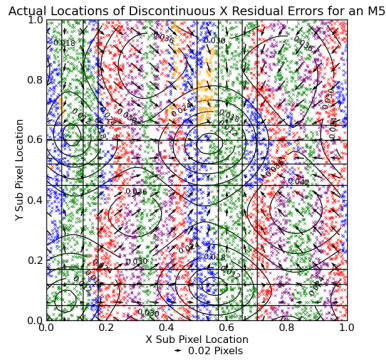
Figure 6: Residual Pixel Errors vs. Sub-Pixel Location in X and Y for a 20s Exposure of a 12th magnitude O5, F5, and M5



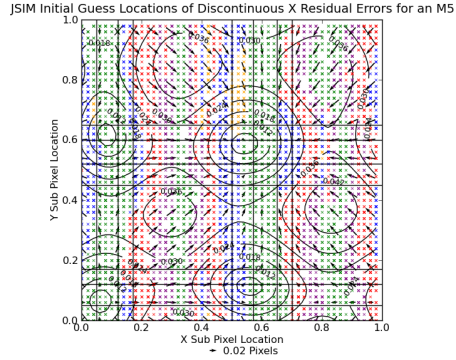
(a)



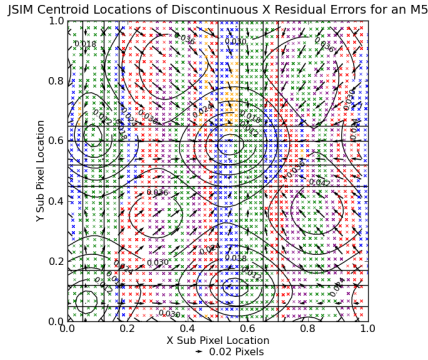
(b)



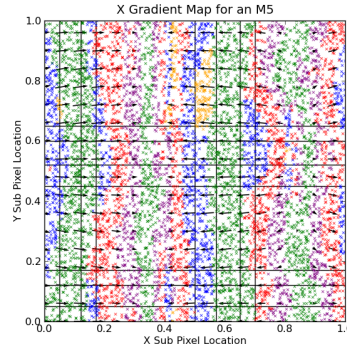
(c)



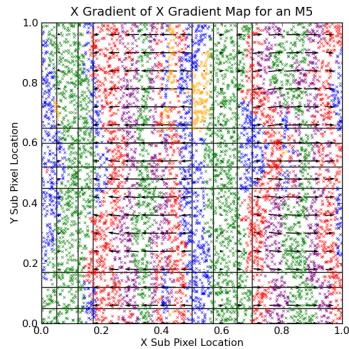
(d)



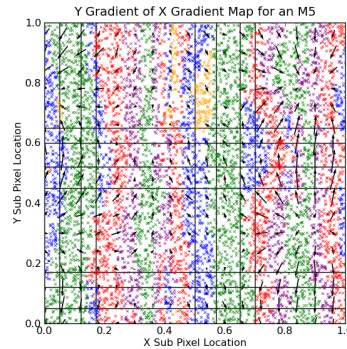
(e)



(f)



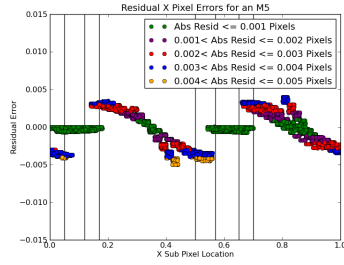
(g)



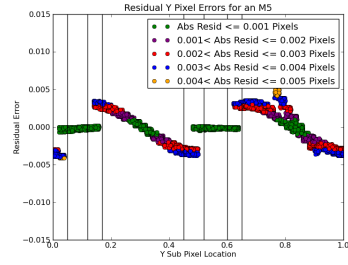
(h)

Figure 7: Investigations on Residual X Pixel Error

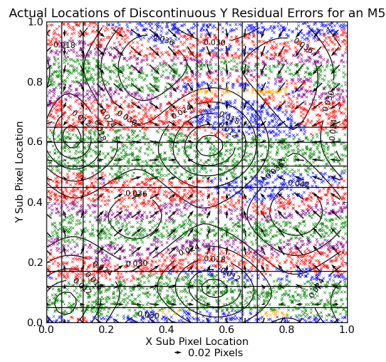
Above we show the residual X and Y pixel errors color coated as a function of error value in (a) and (b), respectively, with discontinuities highlighted by vertical channels also shown in plots (c)-(h). Overplot the pixel offset map, in the same colors as a function of error value, we show the actual pixel locations, JSIM initial guess pixel locations, and final JSIM centroided pixel locations of the residual X pixel errors in (c), (d), and (e) respectively. We also show the gradient map of the X pixel offsets, the X gradient map of the X gradient map, and the Y gradient map of the X gradient map in (f), (g), and (h), respectively.



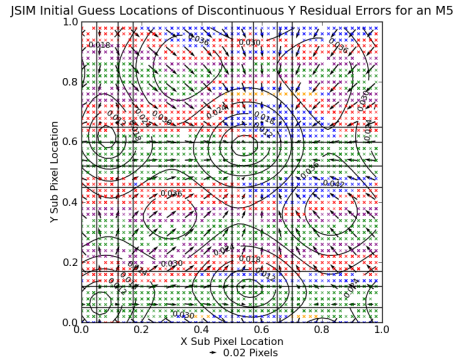
(a)



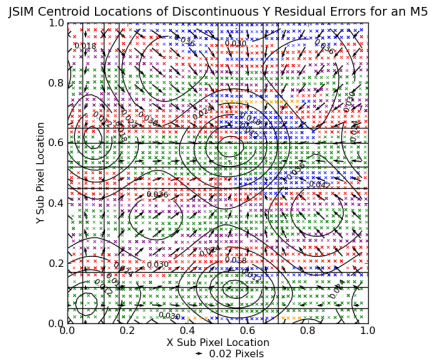
(b)



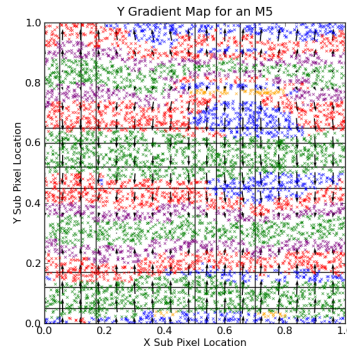
(c)



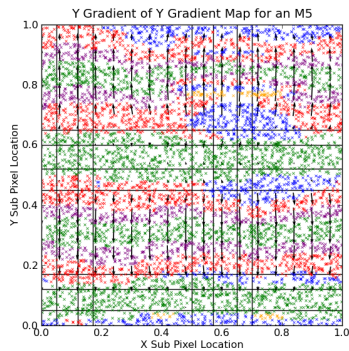
(d)



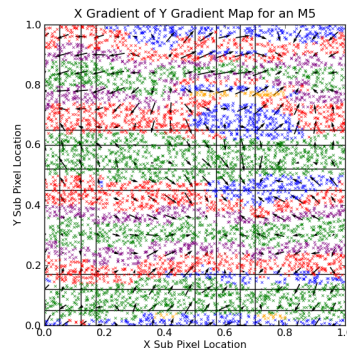
(e)



(f)



(g)



(h)

Figure 8: Investigations on Residual Y Pixel Error

Above we show the residual X and Y pixel errors color coated as a function of error value in (a) and (b), respectively, with discontinuities highlighted by vertical channels also shown in plots (c)-(h). Overplot the pixel offset map, in the same colors as a function of error value, we show the actual pixel locations, JSIM initial guess pixel locations, and final JSIM centroided pixel locations of the residual Y pixel errors in (c), (d), and (e) respectively. We also show the gradient map of the Y pixel offsets, the X gradient map of the Y gradient map, and the Y gradient map of the Y gradient map in (f), (g), and (h), respectively.

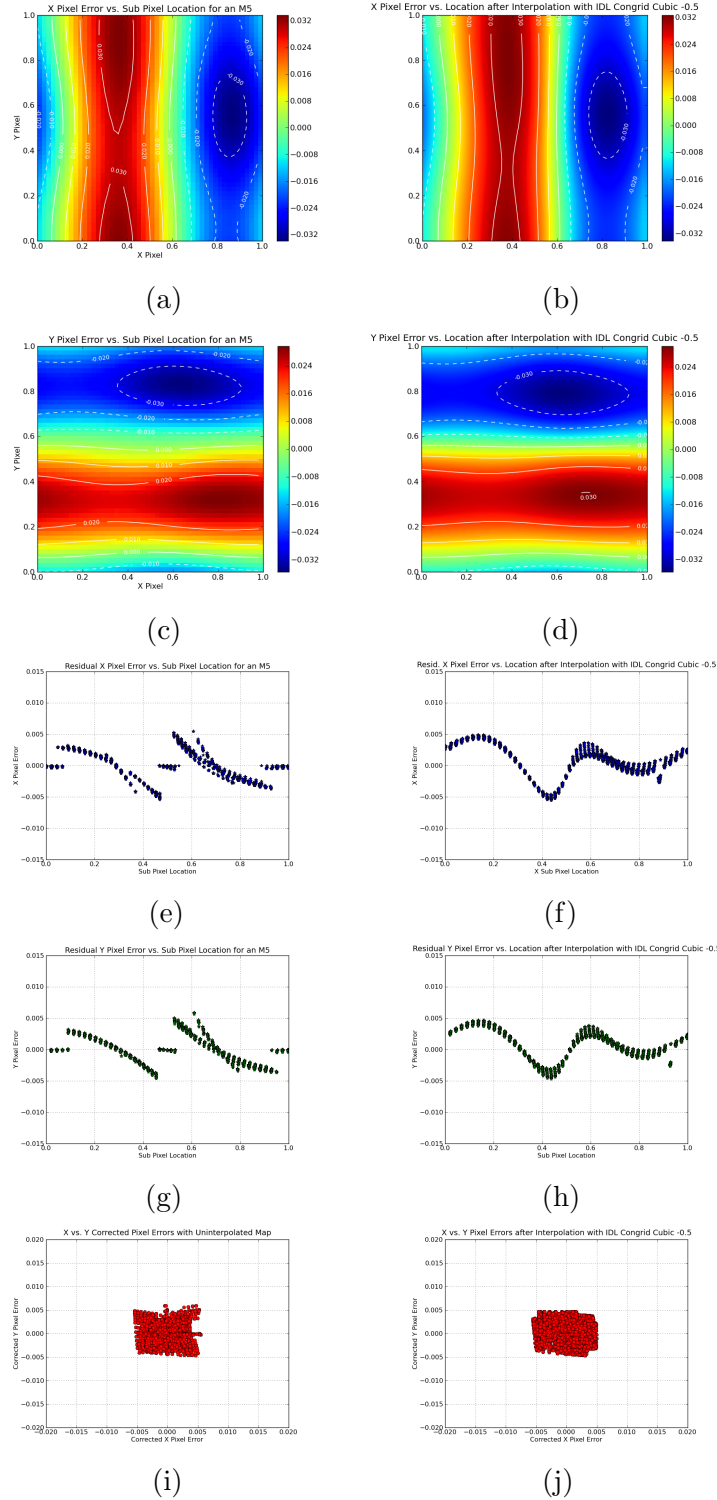
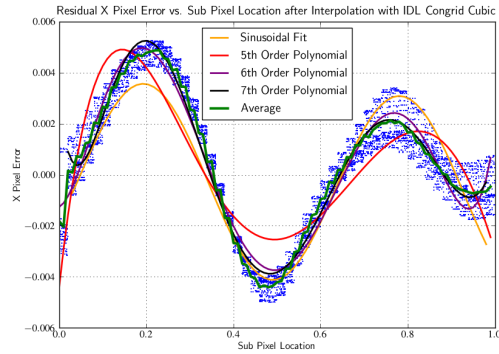
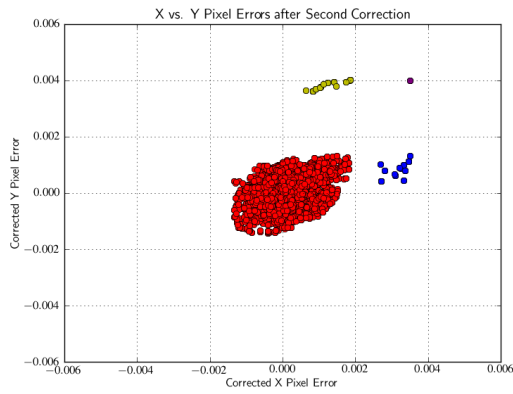


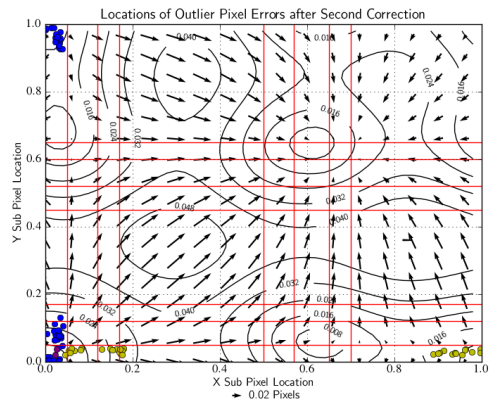
Figure 9: Pixel Error Maps, Interpolated Pixel Error Maps, and Results
 In (a) and (b), we show the X pixel error map and the X pixel error map interpolated with IDL Congrid with the Cubic Parameter = -0.5. In (c) and (d), we show the Y pixel error map and the interpolated Y pixel error map. In (e)-(h), we show the residual X and Y pixel errors after correction with the uninterpolated and interpolated pixel error maps. In (i) and (j), we show the pixel errors before and after interpolation.



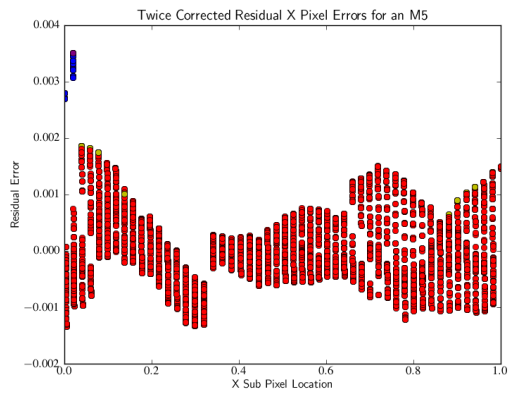
(a)



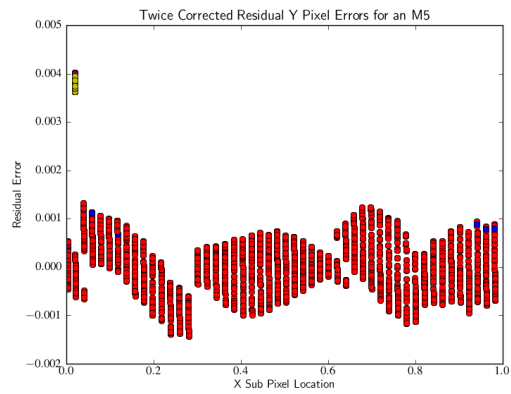
(b)



(c)



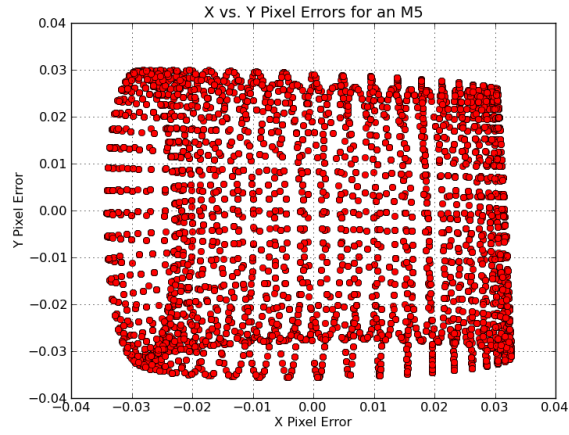
(d)



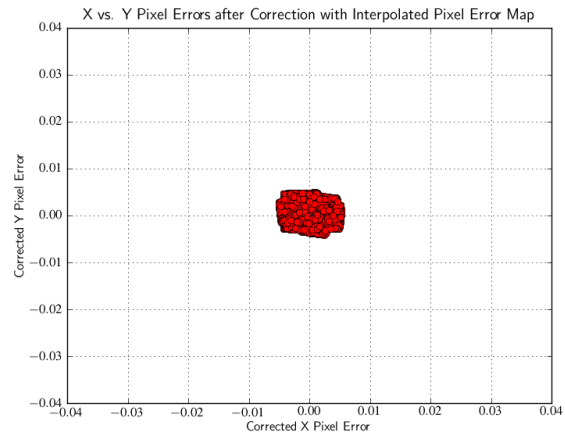
(e)

Figure 10: Second PPE Correction and Result

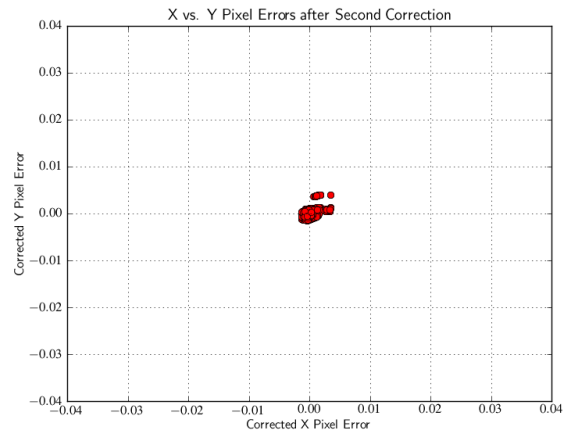
In (a), we show the residual pixel error after correction with the interpolated pixel error maps along with sinusoidal, average, and 5th, 6th, and 7th order polynomial fits. In (b), we show the residual pixel errors after second correction with the average fit, color coated by second residual error pixel location. In (c), in the same colors, we show the actual pixel locations of the outlier second residual pixel error locations. In (c) and (d), in the same colors, we show the X and Y second residual pixel errors as a function of sub pixel location.



(a)



(b)



(c)

Figure 11: Reduction in Pixel Errors

Uncorrected Pixel Errors for a 20s Exposure of a 12th magnitude M5 in (a), Residual Pixel Errors after Correction with Interpolated Pixel Error Map in (b), and Residual Pixel Errors after Correction with Interpolated Pixel Error Map and Average Residual Error Function in (c).

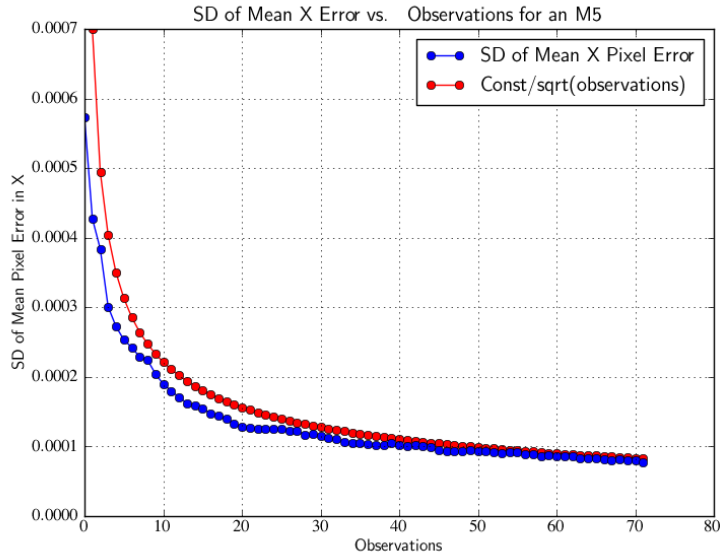


Figure 12: Standard Deviation of Mean X Pixel Error
Standard Deviation of Mean X Pixel Error falls as $1/\sqrt{\#observations}$.